

A Fermi Surface Descriptor Quantifying the Correlations between Anomalous Hall Effect and Fermi Surface Geometry

Elena Derunova^{1,6†}, Jacob Gayles², Yan Sun³, Michael W. Gaultois⁴, and Mazhar N. Ali^{5,6}

¹ Leibniz Institute for Solid State and Materials Research IFW Dresden, Germany

² University of South Florida, Tampa, Florida, USA

³ Max Planck Institute for Chemical Physics of Solids, Dresden, Germany

⁴Leverhulme Research Center for Functional Materials Design, The Materials Innovation Factory, University of Liverpool, Liverpool, UK

⁵Delft University of Technology, Delft, Netherlands

⁶ Max Plank Institute of Microstructure Physics, Halle, Germany

† derunova-el@mail.ru

Abstract

In the last few decades, basic ideas of topology have completely transformed the prediction of quantum transport phenomena. Following this trend, we go deeper into the incorporation of modern mathematics into quantum material science focusing on geometry. Here we investigate the relation between the geometrical type of the Fermi surface and Anomalous and Spin Hall Effects. An index, \mathbb{H}_F , quantifying the hyperbolic geometry of the Fermi surface, shows a universal correlation ($R^2 = 0.97$) with the experimentally measured intrinsic anomalous Hall conductivity, of 16 different compounds spanning a wide variety of crystal, chemical, and electronic structure families, including those where topological methods give $R^2 = 0.52$. This raises a question about the predictive limits of topological physics and its transformation into a wider study of bandstructures' and Fermi surfaces' geometries, opening horizon for prediction of phenomena beyond topological understanding.

Copyright attribution to authors.

This work is a submission to SciPost Physics.

License information to appear upon publication.

Publication information to appear upon publication.

Received Date

Accepted Date

Published Date

Contents

1	Introduction	2
2	Semiclassical dynamics and Fermi surface geometry	3
3	Results	4
3.1	Hyperbolicity Index \mathbb{H}_F and Anomalous Hall Conductivity (AHC)	4
3.2	Correlation-based prediction of AHC: Multiple-EBR Fermi Surface	6
4	Discussion and Conclusion	7
	References	9

1 Introduction

Topological materials have garnered significant attention in recent years for their remarkable electronic properties, which have opened new horizons in condensed matter physics and electronic device engineering [1]. Among other effects, they exhibit anomalous Hall effect (AHE), i.e. additional orthogonal Hall current, which is unexpected from the classical electromagnetic theory perspective. There are various contributions to the AHE, but in this work, we only consider the intrinsic one, which is AHE generated by the internal magnetism combined with the topological connectivity of the electronic eigenstates ψ_{nk} [2]. The accurate prediction of Anomalous Hall Conductivity (AHC), quantifying AHE in materials, especially within the realm of topological materials, relies upon sophisticated computational methodologies. These methods are rooted in the computation of Berry curvature $\Omega(\mathbf{k})$, a fundamental concept in condensed matter physics that offers insights into the geometric phase acquired by electron wavefunctions as they traverse the Brillouin zone. This enables accurate predictions of AHC by establishing a clear connection between the topological properties of electronic bands and transport phenomena as follows [2]:

$$\sigma_{xy} = -\frac{e^2}{\hbar} \int_{\text{BZ}} \frac{d^2k}{(2\pi)^2} \Omega_{xy}(\mathbf{k}) f^{\text{Fermi-Dirac}}(\epsilon(\mathbf{k})) \quad (1)$$

Computational procedures to predict AHC typically commence with ab-initio density functional theory (DFT) calculations. These calculations are followed by a projection into Wannier functions, and subsequently, the computation of Berry curvature at each k-point in the Brillouin zone. The Kubo formula, which relies on Berry curvature and integrates over occupied states in k-space, is then employed to predict the AHC [3]:

$$\Omega_{xy,n}^z(\mathbf{k}) = \sum_{m \neq n} \text{Im}[\langle \psi_{nk} | v_x | \psi_{mk} \rangle \times \frac{\langle \psi_{mk} | v_y | \psi_{nk} \rangle}{(\epsilon_{nk} - \epsilon_{mk})^2}] \quad (2)$$

While this approach has made significant strides in comprehending and forecasting the AHC in topological materials, challenges persist in, e.g. algorithmizing the computational procedure or attaining a high degree of accuracy. The accuracy issues appeared e.g. with simple compounds like Ni [4], where prediction gives a significant offset from experimentally observed AHC. There are various reasons for that, but one could be that the current computational method fundamentally does not take into account the possible coexistence of multiple *unconnected sets* of bands at the Fermi level, as was recently presented in topological quantum chemistry as multi-EBR bandstructures [5]. A more crucial factor for the numerical simulation of quantum effects like AHE is a pressing need to streamline the computational complexity of these calculations to enable high-throughput performance and online execution within materials databases. A possible key avenue for achieving this computational streamlining can be found in consideration of the Fermi surface (FS), representing the locus of states with the highest occupied energy levels, which is fundamental in shaping electronic transport phenomena.

However, a significant challenge arises in the fact that the topological connectivity described by Berry curvature is typically regarded as an intrinsic property of eigenstates and is not readily expressible solely through the distribution of eigenvalues.

In this context, our paper introduces a groundbreaking Fermi surface descriptor \mathbb{H}_F related to the density of hyperbolic points on the Fermi surface, which computation does not include any topological quantities, but only Fermi surface data. It shows higher accuracy in predicting the AHC compared to current methods and unlike them can be simply integrated into material databases. This empirically developed index correlates extremely well with experimentally measured values of intrinsic anomalous Hall conductivity (AHC) ($R^2 = 0.97$, whereas current methods gives just $R^2 = 0.52$). \mathbb{H}_F is tested on 16 different real materials that broadly range from conventional ferromagnets to Weyl semimetals, including cases like Ni and Co_2MnAl , where the Berry phase approach (via the Kubo formalism) does not represent a complete picture of the transport. We found that 13 of the compounds have one EBR FSs and that the limit of the AHC for a single EBR FS is $\approx 1570 \frac{\hbar}{e} (\Omega\text{cm})^{-1}$. Two of the materials examined here, CrPt_3 and Co_2MnAl , have multi-EBR Fermi surfaces and subsequently break the apparent AHC limit. We also find that the \mathbb{H}_F matches predictions of the spin Hall conductivity (SHC) for Pt, Beta-W, and TaGa_3 . The \mathbb{H}_F index also enables an inexpensive and rapid computational prediction of AHE/SHE materials and can be implemented with existing density functional theory (DFT) methods and databases.

Our research represents a significant advancement in the field of topological materials, offering a valuable tool for both theoretical investigations and practical applications. We anticipate that this novel Fermi surface descriptor will not only deepen our understanding of the AHC but also open new avenues for engineering topological materials with tailored electronic and transport properties. The ensuing sections of this paper will detail the development and application of this descriptor, presenting compelling evidence of its enhanced predictive accuracy and its potential to revolutionize the field of topological materials research and its diverse technological applications.

2 Semiclassical dynamics and Fermi surface geometry

In our study, we rely on a semiclassical approach, which helps to understand how electrons move when subjected to electric (\mathbf{E}) and magnetic (\mathbf{B}) fields. Applied fields generate dynamics in the momentum space described by the following equation [6]:

$$\frac{d}{dt}(\hbar\mathbf{k}) = -e \left(\mathbf{E} + \frac{1}{\hbar} \mathbf{v} \times \mathbf{B} \right) \quad (3)$$

Since \mathbf{v} in this equation is the electron's velocity, which is a normal vector to the Fermi surface, the magnetic field generates dynamics on the Fermi surface that lead to the existence of so-called cyclotron orbits around the FS (see figure 1 left). Thus, the shape of the FS must influence the dynamic in the magnetic field described by the equation 3 and, hence, it should affect the AHC.

From that perspective the "shape" of the Fermi surface can be fundamentally classified only into 3 types: elliptic, planar, and hyperbolic, representing positive, zero, and negative Gaussian curvature of the surface correspondingly [7] (see figure 1). If we denote $\boldsymbol{\tau} = \mathbf{v} \times \mathbf{B}$, the \mathbf{B} generated dynamics on the Fermi surface can be simply written as follows:

$$\frac{d}{dt}\mathbf{k} = -\frac{e}{\hbar^2} \boldsymbol{\tau} \quad (4)$$

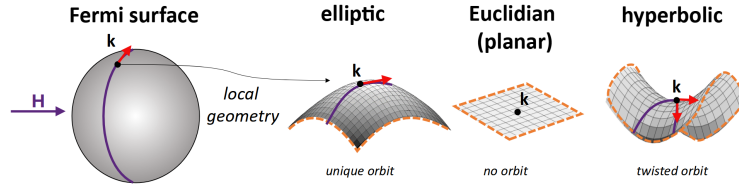


Figure 1: (color online): Local Fermi surface geometry and Fermi surface orbits in the magnetic field

These types of equations are known as dynamical systems and have been extensively studied. Notably, it has been discovered that dynamical systems on hyperbolic surfaces exhibit a property known as ergodicity [8]. In simple terms, over a sufficiently long time, the orbits cover the entire hyperbolic surface, and the dynamics on these surfaces become chaotic. This behavior arises from the stochastic nature of the dynamics, which is rooted in the orbits' intersection in the hyperbolic points, leading to uncertainties in the choice of the orbit. (see figure 1 right).

From the physical perspective, such "mixing" of orbits is close to the idea of non-adiabatic evolution of the eigenstates under the perturbation of the Hamiltonian (e.g. H-field). This non-adiabatic process can possibly result in the anomalous Hall current, similar to how it appears under non-adiabatic evolution due to the Berry curvature. However, it is important to note that ergodic dynamics have only been rigorously established for systems exhibiting a constant negative curvature, a condition not typically met by the Fermi surfaces of real materials, which often possess varying curvatures. Nevertheless, it is reasonable to speculate that regions of hyperbolic curvature within the Fermi surface may undergo non-adiabatic evolution under the influence of an applied magnetic field, giving rise to anomalous Hall currents. By considering that maximal anomalous Hall effect (AHE) occurs in the fully hyperbolic constant curvature surface and that no AHE is expected in fully elliptic constant curvature surface, which is the Fermi sphere of a free electron gas, we propose a hypothesis suggesting that the proportion of hyperbolic to total area within the Fermi surface could serve as an indicator of the magnitude of the AHE.

3 Results

3.1 Hyperbolicity Index \mathbb{H}_F and Anomalous Hall Conductivity (AHC)

To more rigorously quantify the correlation between hyperbolic regions on the FS and AHE/SHE in a chosen direction we introduce the index of the concentration of the hyperbolic areas of the FS, which we denote by \mathbb{H}_F and define as the following:

$$\mathbb{H}_F = \frac{\sum_{\text{hyperbolic points}} I_n |\sin \alpha|}{\sum_{FS} |\sin \alpha|} \quad (5)$$

Where α , is an angle between tangent plane to the FS and AHE plane, and I_n is the sign of the $\partial^2 \epsilon_n / \partial^2 \mathbf{k}$ at the BZ boundary in the Hall current direction. The angle between the tangent plane and the AHE plane indicates effect on the direction of AHE, considering that AHE is maximum when the splitting of orbits happens in the orthogonal to the applied field plane. As defined, \mathbb{H}_F can have a maximum of "1" which means that the entire FS would be hyperbolic, except for the points where the tangent plane is orthogonal to the AHE plane.

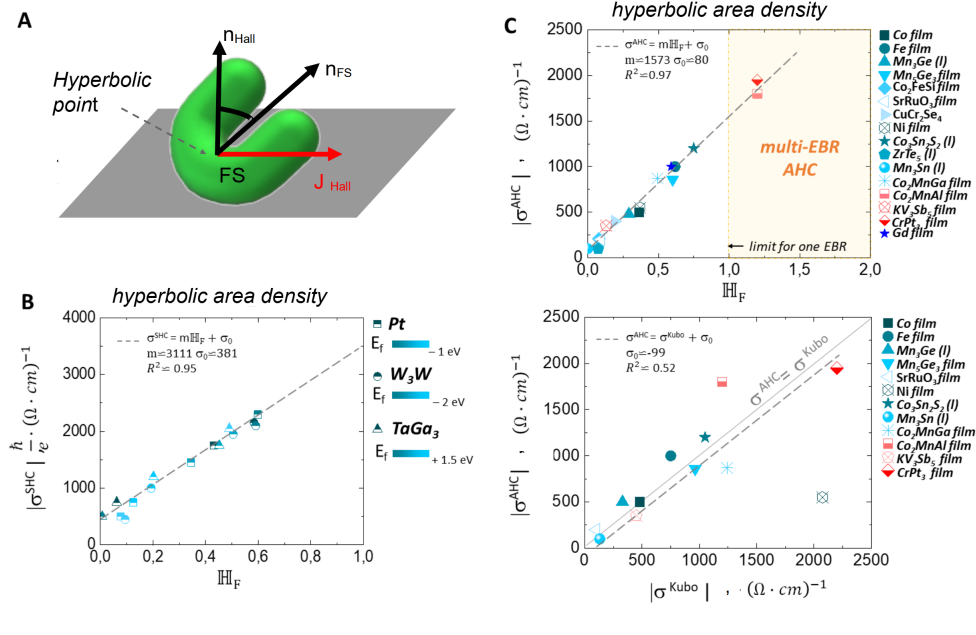


Figure 2: (color online): A. Schematic image of the \mathbb{H}_F calculation in the direction of Hall measurement. B. Correlation graph of the predicted SHC values via the Kubo formalism vs \mathbb{H}_F , as defined in the text. C. Correlation graph top: *experimentally* determined intrinsic AHC vs \mathbb{H}_F for various 2D or layered materials (l identifies layered structures). Bottom: *experimentally* determined intrinsic AHC vs predicted values of AHC via the Kubo formalism.

We performed unperturbed DFT calculations of 16 compounds for which intrinsic AHC values were rigorously experimentally determined [9–17], covering a variety of structural families (perovskites, Heuslars, Kagome lattices, FCC lattices, etc.) and topological classes (Dirac/Weyl/Trivial metals and semimetals). We compared those experimental AHC values to our calculated \mathbb{H}_F (taking care to align the directions of calculation with the directions of measurement for each material in the various experiments). Since, for now, the \mathbb{H}_F parameter is defined for a 2D conductance, we made a comparison of the calculated \mathbb{H}_F with the measured values for thin films or layered structures where the contribution of the third dimension to the total effect is relatively weak.

The result, shown in figure 2, shows an extraordinary linear correlation of the concentration of hyperbolic areas of the FS with the experimentally measured AHC values of all compounds, regardless of structural family or topological class, with an R^2 value of 0.97. Importantly, we also plot the experimentally measured intrinsic AHC values versus the calculated AHC values using the Kubo formalism (based on Berry curvature [4, 9, 12–16]) for the same compounds (Figure 3d). The R^2 drops down to only 0.52, with a few exceptionally inaccurate cases like Co_2MnAl or Ni, where the error is large and the reason is still under investigation [18]. Even without taking those two compounds into account, the R^2 from the Kubo calculated AHCs only rises to 0.87; significantly worse than the \mathbb{H}_F -dependence. We made a similar calculation for SHE compounds, but due to a paucity of experimental data, we are forced to plot the comparison of the Kubo predicted SHC values for Pt, W_3W [3, 19] and $TaGa_3$ (See figure S11 in supplement) at different E_f -levels against their corresponding \mathbb{H}_F values in Figure 3b. This graph also shows a strong correlation of the concentration of hyperbolic areas with the Kubo calculated SHCs with an R^2 of about 0.95, implying that the Kubo approach and the FS-GE approach match well in the case of highly uncompensated FS's [20]; a direction of future investigation.

3.2 Correlation-based prediction of AHC: Multiple-EBR Fermi Surface

From the correlation in figure 2, it can be seen that in the limit of $\mathbb{H}_F = 1$, the intrinsic AHC is expected to reach a maximum value of $1570 \frac{\hbar}{e} (\Omega \text{cm})^{-1}$. However, there are two compounds (Co_2MnAl and CrPt_3) that have \mathbb{H}_F and intrinsic AHCs greater than these maxima. While at first this appears to be an inconsistency, the limit on \mathbb{H}_F can be broken if we take into account the EBR (elementary band representation) for the bands forming FS. Recently it was shown that all bands can be grouped into sets that correspond to distinct EBRs; topological semimetal behavior can be understood as a property of a partially occupied set of such bands (see supplement sections 1 and 2 for more on manifolds and EBRs). Also, the non-quantized contribution to the AHE, as shown by Haldane et al [21], is expected to be a pure Fermi surface property. Combining these two ideas, a part of the FS that is comprised of multiple pockets created by the bands belonging to a single EBR, can be considered distinctly from *another part* of the FS similarly corresponding to the *bands from another EBR*.

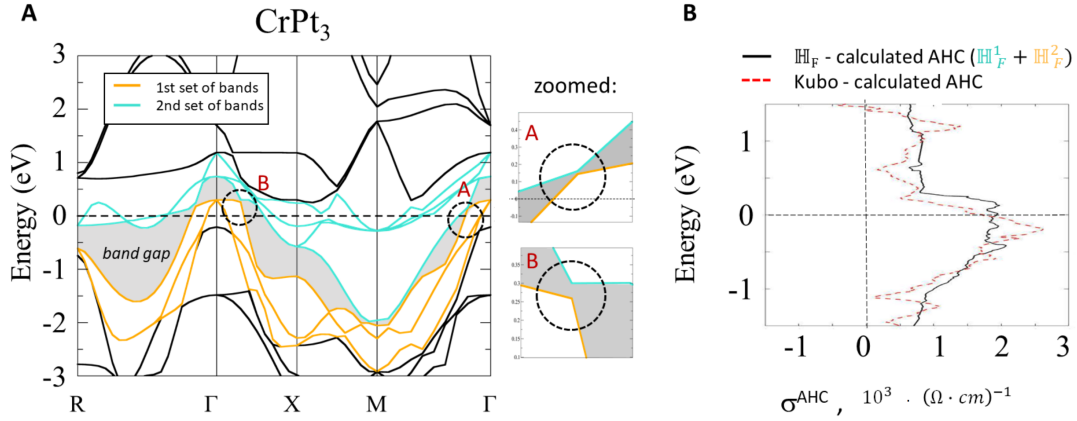


Figure 3: (color online):A. Bandstructure of CrPt_3 . Blue and yellow colors represent two topologically disconnected (having different EBRs) sets of bands crossing the Fermi level. These sets are disconnected by the continuous gap present between them; i.e. true semimetallic behavior. B. Graph of energy resolved AHC predicted in two different ways: red dashed line is the Kubo based prediction, black dashed line stems from the linear correlation between \mathbb{H}_F and AHC calculated separately for FS contributions from each set of bands, then summed together for total \mathbb{H}_F .

In the common case where there is a continuous gap disconnecting sets of bands contributing to the FS, \mathbb{H}_F can be calculated separately using formula 5 for parts of the surfaces arising from distinct sets of bands (bands with differing EBRs), essentially dividing the manifold into submanifolds by EBR, and subsequently summed together in order to characterize the entire FS. This is exactly the case for Co_2MnAl , CrPt_3 and KV_3Sb_5 . For the case of KV_3Sb_5 , it can be seen that the contributions of the distinct EBRs are not cooperative, resulting in a relatively low \mathbb{H}_F of 0.14. However, for Co_2MnAl and CrPt_3 , both have cooperative contributions and correspondingly have \mathbb{H}_F values larger than 1 as well as AHC values larger than $1570 \frac{\hbar}{e} (\Omega \text{cm})^{-1}$; but they still correlate extremely well with the overall trend in Figure 3c

Figure 3a showcases the detailed bandstructure for CrPt_3 with each distinct set of bands colored (blue and yellow) with the continuous gap shaded in gray. The insets clarify the almost-degeneracies near Gamma which are actually gapped. In the Berry curvature approach, the states from the different EBRs are mixed in the total calculation in the Kubo formula. figure 3 b shows the energy dependent AHC calculated from the Kubo formalism as well as the energy

dependent AHC (using the AHC vs \mathbb{H}_F correlation $\sigma = m\mathbb{H}_F + \sigma_0$ to convert \mathbb{H}_F to a numerical AHC value). The results from the two methods are qualitatively similar, but the \mathbb{H}_F result has a slightly better quantitative match to experiment.

4 Discussion and Conclusion

Why does the \mathbb{H}_F method appear to fare better than the Kubo approach for these materials and properties? This is a wide area of future investigation, however, there are few important considerations we elaborate on here. Firstly, the \mathbb{H}_F has a different theoretical motivation and can capture something beyond Berry curvature method, e.g. related to the quantum geometry effects [22]. Besides that, the Kubo formalism looks at the Berry curvature in a point-wise fashion without consideration of their connections to each other, and incorporates a fictitious broadening parameter that does not fully capture finite temperature effects to the electronic structure. Looking at independent points in momentum space means that if a particular point of importance is missed (because of, for example, a very sharp feature or a too low resolution \mathbf{k} -mesh grid), its entire contribution is missed and the calculation can become inaccurate. This is fundamentally different than the *path-wise* \mathbb{H}_F method which looks at points and their connections to each other because it is approximating trajectories. This is likely related to the \mathbb{H}_F plateaus (see figure 4) at relatively sparse K-meshes of $\approx 30 \times 30 \times 30$, unlike the typical $> 150 \times 150 \times 150$ \mathbf{k} -mesh grids used in the Kubo analyses (where the \mathbf{k} -mesh must also increase for tightening the broadening factor). Secondly, the \mathbb{H}_F calculations rely purely on the first principles calculation of the Fermi Surface and not an interpolated/tight-binding representation of the first principles calculation as in Kubo. This (i) eliminates the need for Wannier/tight-binding Hamiltonians which loses the gauge invariance in the convergence process, and (ii) \mathbb{H}_F calculations are not restrained by the quality of the Wannier fit which are localized functions that will always have trouble capturing the completely de-localized topological states present in some systems. Finally, and perhaps most importantly, the Kubo formalism looks at two-band intersections, not multiband intersections, meaning it ignores higher order intersections that can also result in anomalous transport contribution. The \mathbb{H}_F method inherently looks at *n-band intersections* since it is a pure Fermi Surface analysis method and the Fermi Surface (and its features) is made up of any number of bands crossing E_F .

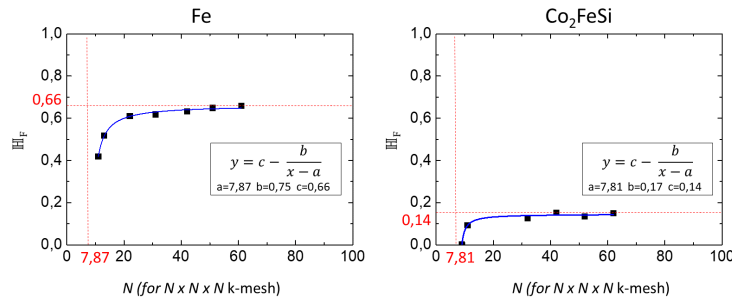


Figure 4: (color online): \mathbb{H}_F dependence of k-mesh density for Fe and Co_2FeSi . y-axis is the calculated total \mathbb{H}_F , and the x-axis is k-points cubed.

When compared with the current Berry curvature driven method for AHE/SHE prediction via the Kubo formalism, the \mathbb{H}_F index is also, computationally, a much simpler metric as it requires just basic DFT calculation without Wannier projection, and thus can be carried out at a significant reduction in time and cost. Importantly, this analysis method can easily be fully automated and implemented into material databases, and can enable artificial intelligence and machine learning based searches of large repositories of compounds for materials with

desirable traits for technological applications. For now the \mathbb{H}_F index is still a relatively rough estimation and also is limited to the cases of 2D materials. However, the numerical correlation of the AHE/SHE with \mathbb{H}_F of $R^2 = 0.97$ proves that the concept of using geometric classification is not just a "blue-sky" theoretical research effort; it has immediate applications to outstanding questions in condensed matter physics.

Important future work includes exploring the full theoretical motivation of the method and its relation to the quantum geometry metric (Fubini-Study Metric) [22] for the rigorous transport theory as well as finding correlations between other geometrical classes of FS regions and other quantum transport phenomena. The other direction could be to study, how boundaries between FS regions interact and how they may result into effectively turbulent quasi-particle dynamics. Broadly, the concepts outlined here will alter the current paradigm of understanding the non-trivial transport regimes (like AHE/SHE) moving it to include geometrical properties of the FS, rather than just topological properties of the eigenstates of the Hamiltonian.

In summary, we have introduced the idea of non-ergodicity of the FS orbits on the hyperbolic regions, that might result in the non-adiabatic evolution of the eigenstates and corresponding transport effects. This concept has been applied to develop a simple index, \mathbb{H}_F , for quantifying the contribution of the concentration of hyperbolic areas, and showed a universal correlation ($R^2 = 0.97$) with experimentally measured intrinsic AHE values for 16 different compounds spanning a wide variety of crystal, chemical, and electronic structure families. An apparent maximum value, at $\mathbb{H}_F = 1$, of $1570 \frac{\hbar}{e} (\Omega \text{cm})^{-1}$ was determined for materials with an FS created by bands belonging to a single EBR; materials with multi-EBR FS's can, and do, break this limit as evidenced by CrPt_3 and Co_2MnAl . Use of the \mathbb{H}_F index allows direct calculation of the AHE/SHE at a much lower computational cost than current methods by eliminating the need for Wannier projection and can be implemented with existing high throughput DFT methods and databases. This work highlights the importance of, and opportunities laying ahead for, developing a complete theory of *geometrical understanding* of electronic structure manifolds beginning with Fermi surfaces. Also, these ideas can be extended to bosonic (e.g. magnonic) band structures and their constant energy momentum surfaces as well. In analogy to the broad impact that topological understanding of these structures had, a geometry incorporated in it will lead to a deeper understanding of at least electron transport and have far-reaching consequences in condensed matter physics.

Acknowledgements

Author contributions E.D. was the lead researcher on this project. She carried out the main theoretical derivations as well as the majority of the calculations and analysis. Y.S., M.G. and J.G. assisted with calculations and interpretation. M.N.A and E.D. are the principal investigators.

Funding information This research was supported by the Alexander von Humboldt Foundation Sofia Kovalevskaja Award and the BMBF MINERVA ARCHES Award. E.D. thanks O. Janson and Y. Blanter for the productive discussions and support on this work. M.W.G. thanks the Leverhulme Trust for funding via the Leverhulme Research Centre for Functional Materials Design.

References

- [1] B. A. Bernevig, *Topological Insulators and Topological Superconductors*, Princeton University Press, Princeton, ISBN 9781400846733, doi:[doi:10.1515/9781400846733](https://doi.org/10.1515/9781400846733) (2013).
- [2] D. Xiao, M.-C. Chang and Q. Niu, *Berry phase effects on electronic properties*, Rev. Mod. Phys. **82**(3), 1959 (2010).
- [3] M. Gradhand, D. Fedorov, F. Pientka, P. Zahn, I. Mertig and B. Györfly, *First-principle calculations of the berry curvature of bloch states for charge and spin transport of electrons*, Journal of Physics: Condensed Matter **24**(21), 213202 (2012).
- [4] X. Wang, D. Vanderbilt, J. R. Yates and I. Souza, *Fermi-surface calculation of the anomalous hall conductivity*, Phys. Rev. B **76**, 195109 (2007), doi:[10.1103/PhysRevB.76.195109](https://doi.org/10.1103/PhysRevB.76.195109).
- [5] B. Bradlyn, L. Elcoro, J. Cano, M. G. Vergniory, Z. Wang, C. Felser, M. I. Aroyo and B. A. Bernevig, *Topological quantum chemistry*, Nature **547**, 298 EP (2017), Article.
- [6] N. Ashcroft and D. Mermin, *Solid State Physics*, Brooks and Cole (1976).
- [7] V. Toponogov and V. Rovinski, *Differential Geometry of Curves and Surfaces: A Concise Guide*, Birkhauser Boston, ISBN 9780817644024 (2006).
- [8] D. V. Anosov, *Geodesic flows on closed riemannian manifolds of negative curvature*, Jour Proc. Steklov Inst. Math. **90**, 1 (1967).
- [9] E. Liu, Y. Sun, N. Kumar, L. Muechler, A. Sun, L. Jiao, S.-Y. Yang, D. Liu, A. Liang, Q. Xu, J. Kroder, V. Süß *et al.*, *Giant anomalous Hall effect in a ferromagnetic kagome-lattice semimetal*, Nature Physics **14**(11), 1125 (2018), doi:[10.1038/s41567-018-0234-5](https://doi.org/10.1038/s41567-018-0234-5).
- [10] T. Miyasato, N. Abe, T. Fujii, A. Asamitsu, S. Onoda, Y. Onose, N. Nagaosa and Y. Tokura, *Crossover Behavior of the Anomalous Hall Effect and Anomalous Nernst Effect in Itinerant Ferromagnets*, Physical Review Letters **99**(8) (2007), doi:[10.1103/PhysRevLett.99.086602](https://doi.org/10.1103/PhysRevLett.99.086602).
- [11] A. K. Nayak, J. E. Fischer, Y. Sun, B. Yan, J. Karel, A. C. Komarek, C. Shekhar, N. Kumar, W. Schnelle, J. Kübler, C. Felser and S. S. P. Parkin, *Large anomalous Hall effect driven by a nonvanishing Berry curvature in the noncolinear antiferromagnet Mn_3Ge* , Science Advances **2**(4), e1501870 (2016), doi:[10.1126/sciadv.1501870](https://doi.org/10.1126/sciadv.1501870).
- [12] J. Kübler and C. Felser, *Weyl Fermions in antiferromagnetic Mn_3Sn and Mn_3Ge* , EPL (Europhysics Letters) **120**(4), 47002 (2017), doi:[10.1209/0295-5075/120/47002](https://doi.org/10.1209/0295-5075/120/47002), ArXiv: 1711.03891.
- [13] C. Zeng, Y. Yao, Q. Niu and H. H. Weitering, *Linear Magnetization Dependence of the Intrinsic Anomalous Hall Effect*, Physical Review Letters **96**(3) (2006), doi:[10.1103/PhysRevLett.96.037204](https://doi.org/10.1103/PhysRevLett.96.037204).
- [14] Z. Fang, N. Nagaosa, K. S. Takahashi, A. Asamitsu, R. Mathieu, T. Ogasawara, H. Yamada, M. Kawasaki, Y. Tokura and K. Terakura, *The anomalous hall effect and magnetic monopoles in momentum space*, Science **302**(5642), 92 (2003), doi:[10.1126/science.1089408](https://doi.org/10.1126/science.1089408), <https://science.sciencemag.org/content/302/5642/92.full.pdf>.

- [15] I. Imort, P. Thomas, G. Reiss and A. Thomas, *Anomalous Hall effect in the Co-based Heusler compounds Co_2FeSi and Co_2FeAl* , *Journal of Applied Physics* **111**(7), 07D313 (2012), doi:[10.1063/1.3678323](https://doi.org/10.1063/1.3678323).
- [16] J.-C. Tung and G.-Y. Guo, *High spin polarization of the anomalous Hall current in Co-based Heusler compounds*, *New Journal of Physics* **15**(3), 033014 (2013), doi:[10.1088/1367-2630/15/3/033014](https://doi.org/10.1088/1367-2630/15/3/033014).
- [17] A. Markou, D. Kriegner, J. Gayles, L. Zhang, Y.-C. Chen, B. Ernst, Y.-H. Lai, W. Schnelle, Y.-H. Chu, Y. Sun and C. Felser, *Thickness dependence of the anomalous hall effect in thin films of the topological semimetal co_2MnGa* , *Phys. Rev. B* **100**, 054422 (2019), doi:[10.1103/PhysRevB.100.054422](https://doi.org/10.1103/PhysRevB.100.054422).
- [18] L. Ye, Y. Tian, X. Jin and D. Xiao, *Temperature dependence of the intrinsic anomalous hall effect in nickel*, *Phys. Rev. B* **85**, 220403 (2012), doi:[10.1103/PhysRevB.85.220403](https://doi.org/10.1103/PhysRevB.85.220403).
- [19] E. Derunova, Y. Sun, C. Felser, S. S. P. Parkin, B. Yan and M. N. Ali, *Giant intrinsic spin Hall effect in W_3Ta and other A15 superconductors*, *Science Advances* **5**(4) (2019), doi:[10.1126/sciadv.aav8575](https://doi.org/10.1126/sciadv.aav8575), <https://advances.sciencemag.org/content/5/4/eaav8575.full.pdf>.
- [20] A. Hoffmann, *Spin hall effects in metals*, *IEEE Transactions on Magnetics* **49**(10), 5172 (2013), doi:[10.1109/TMAG.2013.2262947](https://doi.org/10.1109/TMAG.2013.2262947).
- [21] F. D. M. Haldane, *Berry Curvature on the Fermi Surface: Anomalous Hall Effect as a Topological Fermi-Liquid Property*, *Physical Review Letters* **93**(20) (2004), doi:[10.1103/PhysRevLett.93.206602](https://doi.org/10.1103/PhysRevLett.93.206602).
- [22] R. Cheng, *Quantum Geometric Tensor (Fubini-Study Metric) in Simple Quantum System: A pedagogical Introduction* (2010), [1012.1337](https://arxiv.org/abs/1012.1337).